

---

# Using Semantic Distance to Estimate Uncertainty in LLM-Based Code Generation

---

**Weilin He**  
University of Bristol  
te23071@bristol.ac.uk

**Arindam Sharma**  
University of Bristol  
arindam.sharma@bristol.ac.uk

**Cristina David**  
University of Bristol  
cristina.david@bristol.ac.uk

## Abstract

LLMs show strong performance in code generation, but their outputs lack correctness guarantees. Sample-based uncertainty estimators address this by generating multiple candidate programs and measuring their disagreement. However, existing estimators make different design choices about how behaviours are identified, aggregated, referenced and compared, making them difficult to assess. We therefore first introduce a taxonomy that disentangles these choices and reveals a missing design point: *semantic distance-aware uncertainty estimation*, which measures not only whether sampled programs disagree, but how severely their execution behaviours differ. Across LiveCodeBench, MBPP, HumanEval-X and BigCodeBench, spanning Python, Java and C++, our metrics provide strong proxies for correctness, and consistently outperform state-of-the-art sample-based baselines across both closed-source models (GPT-3.5-Turbo, GPT-4o-mini, Gemini-2.5-Flash-Lite, Claude Opus 4.5) and an open-source model (DeepSeek-Coder-V2). The method is practical: it requires neither model internals nor LLM-as-judge calls, remains robust across models, languages, sampling temperatures and fuzzing settings, and reduces runtime by approximately 48–79% relative to existing baselines.

## 1 Introduction

The adoption of Large Language Models (LLMs) in software engineering has been rapid, with the volume of LLM-generated code projected to increase further [6]. As such, the well-known problem of hallucinations now threatens the reliability of critical software systems [19], spurring a growing body of work on assessing the correctness of LLM-generated code [9]. Yet, in many settings, external validation is unavailable or incomplete: generated programs may lack reference implementations or complete test suites [13, 21, 22].

A common reference-free strategy is to estimate uncertainty [14] from *disagreement* across multiple independently sampled outputs. In natural language generation, such methods interpret variation across samples as a signal of epistemic uncertainty [7, 16, 1]. Recent work adapts the same principle to code generation [17, 23, 24], using signals that range from static analysis of program text to dynamic comparison of execution behaviour.

**A four-axis taxonomy of sample-based uncertainty estimators.** Although many uncertainty estimators now exist, they are difficult to compare directly: they combine different notions of equivalence, aggregation, reference behaviour and disagreement. Our first contribution is therefore a taxonomy that makes these choices explicit.

Table 1: Representative sample-based uncertainty estimators positioned along four design axes. *Equiv. proxy* denotes how outputs are represented or grouped into behaviours. *Aggregation* is marginal or pairwise. *Reference* specifies which behaviours are compared for pairwise methods. *Dissimilarity* specifies how compared behaviours are scored; N/A indicates that no pairwise comparison is used.

Method	Equiv. proxy	Aggregation	Reference	Dissimilarity
Semantic Entropy [7, 16]	NL-Entailment	marginal	N/A	N/A
Symbolic equiv. [23]	symbolic execution	marginal	N/A	N/A
Self-Consistency [25]	exact string match	marginal	N/A	N/A
SelfCheckGPT [20]	NL-LLM	pairwise	uniform-pairwise	binary
ChainPoll [8]	LLM voting	pairwise	top1-only	binary
HonestCoder [17]	multi-modal heuristic	pairwise	uniform-pairwise	binary
DiffTrust [24]	execution fuzz	pairwise	top-anchored	binary
EigenScore [18]	NL-Embedding	pairwise	uniform-pairwise	binary
SDE (ours)	execution fuzz	pairwise	uniform-pairwise	graded
DSDE (ours)	execution fuzz	pairwise	top-anchored	graded

At a high level, the methods in Table 1 share a common sample-and-aggregate structure: they sample  $K$  candidate outputs, identify or compare behaviours using some proxy for equivalence, and aggregate the resulting evidence into a scalar uncertainty score. We organise this design space along four axes: *equivalence proxy*, *aggregation structure*, *reference behaviour* and *dissimilarity*.

*Equivalence proxy* specifies how candidate outputs are represented or grouped into behaviours. Existing methods use a range of proxies, including NLI- or LLM-based equivalence judgements [20], syntactic and data-flow heuristics [17], symbolic execution [23], execution-based grouping on shared inputs [24], exact string matching [25], and embedding similarity [18].

*Aggregation structure* specifies whether uncertainty is computed from marginal behaviour probabilities or from pairwise comparisons between behaviours. Marginal methods [7, 23, 25] summarise how probability mass is spread across behaviours, without asking whether two behaviours are semantically close or far apart. Pairwise methods [20, 8, 17, 24, 18], by contrast, explicitly compare behaviours.

*Reference behaviour* applies to pairwise methods and specifies which behaviours are compared. Some methods aggregate over all pairs (*uniform-pairwise*) [20, 17, 18]; some compare the dominant behaviour against alternatives (*top-anchored*) [24]; and some compare only the top-ranked output against alternatives while discarding alternative probabilities (*top1-only*) [8].

*Dissimilarity* applies to pairwise methods and specifies how differences between compared behaviours are scored. Existing pairwise methods use a binary or shallow notion of disagreement: two behaviours either agree or disagree [20, 8, 24]. Marginal methods, such as Semantic Entropy [7], do not use an inter-behaviour dissimilarity at all.

**Limitation of existing methods.** By separating design choices, the taxonomy makes prior methods easier to compare and exposes a key limitation: *existing estimators provide only a coarse account of behavioural difference*. Marginal methods collapse uncertainty to the distribution of mass over behaviours, without asking whether those behaviours are semantically close or far apart. Pairwise methods do compare behaviours, but typically only through a binary or shallow agree/disagree signal. As a result, two programs that differ on one input out of ten may be treated like two programs that disagree on every input. This is a poor abstraction for code, where behavioural differences are often graded [27]. A useful sample-based uncertainty estimator should therefore capture not only whether sampled programs disagree, but also how severely they disagree.

**Our approach.** Our key observation is that programs, unlike free-form natural language, are executable objects. This makes semantic difference directly measurable: two programs can be compared by how often, and in what ways, their executions differ on shared inputs.

We therefore propose *semantic distance-aware uncertainty estimation*. Instead of treating all behavioural disagreements as equally severe, we assign graded dissimilarities between execution behaviours and aggregate them into uncertainty scores. The framework is agnostic to the equivalence proxy: any procedure that identifies behaviourally equivalent programs can be used. In this paper, we

use fuzzing: unlike lightweight static proxies [17], it captures observable program behaviour, while avoiding the substantial cost of more principled static techniques such as symbolic execution [23].

We define two metrics, corresponding to two reference behaviours. SDE uses uniform-pairwise aggregation, grounded in Rao’s quadratic entropy, and measures global behavioural diversity across sampled programs. DSDE uses top-anchored aggregation, measuring how strongly the alternatives disagree with the dominant behaviour containing the top-ranked program. The former is suited to task- or model-level uncertainty, while the latter targets the reliability of the specific output shown to the user.

In summary, the contributions of this paper are as follows:

- We introduce a four-axis *taxonomy of sample-based uncertainty estimators*, making existing methods easier to compare and clarifying which design choices distinguish them.
- We propose *semantic distance-aware uncertainty metrics* as a proxy for correctness in code generation. On *LiveCodeBench*, our metrics achieve *strong discrimination between correct and incorrect solutions*, with AUROC > 0.8.
- We provide extensive evidence of generalisation across benchmarks, languages, models, and sampling regimes. Beyond *LiveCodeBench*, our metrics remain effective on *MBPP* [2], *Big-CodeBench* [29] and *HumanEval-X* [28]; across *Python*, *Java* and *C++*; across closed-source and open-weights models; and under varying task difficulties and sampling temperatures.
- We show that distance-aware uncertainty is *cost-effective* relative to strong state-of-the-art uncertainty estimation baselines: our metrics substantially improve predictive performance while reducing runtime by approximately 48–79%.

## 2 Distance-Aware Uncertainty Measures

We now formalise the three components needed to compute our distance-aware uncertainty scores: semantic clusters, distances between clusters, and the aggregation rules that turn these distances into a scalar uncertainty estimate. The clustering step is not specific to our metric: any procedure that partitions candidate programs into behaviourally equivalent groups can be used. In this paper, we use execution signatures over a shared input set, which provides a simple and practical instantiation.

**Setup: Semantic Clusters.** Given a task description  $d$ , let  $\Pi = \{\pi_1, \dots, \pi_K\}$  be  $K$  candidate programs sampled from a stochastic code-generation model. Let  $\mathcal{I} = (x_1, \dots, x_N)$  be a fixed set of inputs shared across all candidates. Executing a program  $\pi$  on  $\mathcal{I}$  yields its *execution signature*  $\sigma_{\mathcal{I}}(\pi) = (o_1(\pi), \dots, o_N(\pi))$ , where  $o_k(\pi)$  is the observed outcome of  $\pi$  on input  $x_k$ . An outcome is either a normal output value or an abnormal termination labelled by its error type.

Programs are placed in the same semantic cluster iff their execution signatures are identical. Let  $\{C_1, \dots, C_M\}$  be the resulting partition of  $\Pi$ . The empirical cluster probability is  $p_i = \frac{|C_i|}{K}$ , with  $\sum_{i=1}^M p_i = 1$ .

### 2.1 Semantic Distance

We next define a graded distance between semantic clusters. Since all programs in a cluster have the same execution signature on  $\mathcal{I}$ , the distance between two clusters is independent of the choice of representatives. For any  $\pi \in C_i$  and  $\pi' \in C_j$ , the semantic distance between clusters  $C_i$  and  $C_j$  is

$$d_{ij} = \frac{1}{N} \sum_{k=1}^N \delta(o_k(\pi), o_k(\pi')). \quad (1)$$

The per-input outcome distance  $\delta(o, o') \in [0, 1]$  is defined as

$$\delta(o, o') = \begin{cases} 0 & \text{if } o \text{ and } o' \text{ are equal normal outputs,} \\ 1 & \text{if both outcomes are normal and } o \neq o', \\ a & \text{if exactly one outcome is abnormal,} \\ b & \text{if both outcomes are abnormal with different error types,} \\ c & \text{if both outcomes are abnormal with the same error type.} \end{cases} \quad (2)$$

where  $a, b, c \in [0, 1]$  are graded disagreement costs. We treat these values as hyperparameters because abnormal executions do not induce a canonical semantic distance: identical errors may indicate related failure modes, but need not imply behavioural equivalence. We use a fixed default in the main experiments (see §4.1) and assess sensitivity in §4.5.

By construction,  $d_{ij}$  is symmetric, satisfies  $d_{ii} = 0$ , and lies in  $[0, 1]$ .

## 2.2 Uncertainty Metrics

Given semantic clusters  $\{C_1, \dots, C_M\}$ , empirical probabilities  $\{p_1, \dots, p_M\}$ , and pairwise distances  $\{d_{ij}\}$ , we define two distance-aware uncertainty metrics. They share the same clustering and distance definitions, but differ in their anchor: one aggregates globally over all cluster pairs, while the other anchors uncertainty to the cluster containing the top-ranked output.

**Semantic Distance Entropy (SDE).** Our first measure is a symmetric distance-aware estimator inspired by Rao’s quadratic entropy, weighting each cluster pair by the product of cluster probabilities and their semantic distance:

$$SDE = \sum_{i < j} p_i p_j d_{ij}. \quad (3)$$

SDE captures global behavioural diversity: it is large when substantial probability mass is spread across clusters that are far apart in execution behaviour.

**Dominant Semantic Distance Entropy (DSDE).** In deployment, users typically inspect or rely on the model’s top-ranked output [5]. We therefore define a top-anchored variant that measures uncertainty relative to the behaviour that would actually be served. Let  $c^* \in \{1, \dots, M\}$  be the index of the cluster containing the top-ranked program  $\pi_1$ , so that  $C_{c^*} = C(\pi_1)$ . We define

$$DSDE = \sum_{i \neq c^*} p_i d_{c^*, i}. \quad (4)$$

DSDE measures how strongly the alternatives disagree with the top-ranked behaviour, weighted by the empirical probability of each alternative. Unlike SDE, which treats all cluster pairs symmetrically, DSDE is targeted at the reliability of the specific output shown to the user.

## 3 Overview of the Approach

We present an end-to-end evaluation pipeline for execution-based uncertainty estimation in code generation, which consists of four main stages:

**First stage: Candidate program sampling.** Given a programming task described by natural language input  $d$ , let  $\text{Coder}(\cdot)$  denote a code generation system. Without access to reference implementations or model internals, the system independently samples  $K$  candidate programs  $\{\pi_1, \pi_2, \dots, \pi_K\}$ ,  $\pi_k \sim p(\pi \mid d)$ , where each  $\pi_k$  corresponds to the raw code returned by API call.

**Second stage: Fuzzing-based input generation.** Starting from an initial set of valid task inputs, we generate fuzzed inputs using a lightweight, type-aware mutation strategy designed for the heterogeneous input spaces common in code-generation benchmarks. We apply structure-preserving, type-specific mutations iteratively until  $N$  executable fuzzed inputs are obtained, providing behavioural variation for execution-based equivalence and uncertainty estimation.

By default, we follow Valentin et al. [24] and use benchmark-provided test cases as seed inputs. However, our pipeline does not rely on such seeds: in §4.5, we show that a seed-free variant remains effective. We also report input-quality diagnostics for the resulting fuzz suites, including validity, uniqueness, and coverage, in Appendix A.

More generally, the pipeline is *fuzzer-agnostic*: the input-generation component can be replaced by any suitable fuzzing strategy, allowing us to inherit advances from the fuzzing community. For example, in §4.3, we use whitebox fuzzing [10] for BigCodeBench.

**Third stage: Execution-based representation and clustering.** Let  $\mathbf{i} = (i_1, i_2, \dots, i_N)$  denote the set of test inputs associated with the task, where  $N$  is the number of inputs. This input set is shared

across all candidate programs  $\pi = (\pi_1, \pi_2, \dots, \pi_K)$ . Each candidate program  $\pi_k$  is executed on all inputs in  $\mathbf{i}$ , yielding an execution output vector  $\mathbf{o}_k = (\pi_k(i_1), \pi_k(i_2), \dots, \pi_k(i_N))$ .

Candidate programs are clustered according to behavioural equivalence: programs with identical execution signatures are assigned to the same behavioural cluster. For abnormal executions, programs are grouped into the same cluster if they terminate with the same error.

**Fourth stage: Uncertainty computation.** Based on the semantic clusters, we compute SDE and DSDE.

## 4 Experiments

In this section, we will evaluate our distance-aware uncertainty metrics. Our experiments are designed to answer the following questions:

**RQ1 (Predictive Performance).** Do distance-aware uncertainty metrics reliably estimate program correctness, and how do they compare to existing baselines [24, 17, 7]?

**RQ2 (Generalisation).** Do distance-aware uncertainty metrics transfer across benchmarks of varying difficulty and scale, programming languages, sampling temperatures and model families?

**RQ3 (Cost-effectiveness).** Are distance-aware uncertainty metrics cheap enough for inference-time deployment under aggressive sample budgets and competitive against runtime baselines?

**RQ4 (Robustness to design choices).** Do distance-aware uncertainty metrics remain reliable under different design choices, including fixed versus tuned distance weights and the absence of benchmark-provided test inputs?

### 4.1 Experimental Setup

**Models.** We conduct experiments using representative code generation models spanning different capability tiers: GPT-3.5-Turbo (low), GPT-4o-mini (medium), Gemini-2.5-Flash-Lite (medium), and Claude Opus 4.5 (high), with respective *pass@1* success rates of 30.83%, 49.24%, 60.53%, and 82.73% on *LiveCodeBench*. To assess generalisation (§4.3), we additionally use the open-weights model DeepSeek-Coder-V2 (*pass@1* 38.14% on *LiveCodeBench*).

**Datasets.** We evaluate on four complementary benchmarks spanning different task difficulties and programming languages. Our primary benchmark is *LiveCodeBench* (LCB) [15] (Python). To assess generalisation (§4.3), we additionally use *MBPP* [2] (Python), *HumanEval-X* [28] (Python, Java, and C++), and *BigCodeBench* [29] (Python). Detailed statistics and task descriptions are in Appendix C.3.

**Experimental configuration.** Unless otherwise specified, we sample with temperature  $T = 0.6$  following prior code-generation work [17, 11], generate  $K = 10$  candidate programs per task, and evaluate them on  $N = 10$  fuzz inputs with a 0.2 s per-input execution timeout. We use  $(a, b, c) = (1, 0.8, 0.6)$  from §2.1; a sensitivity analysis shows the fixed weights deviate by less than 0.011 AUROC from per-setting learned weights, more details can be found in §4.4. All experiments are run on an Apple M4 Pro with 24 GB of RAM.

**Prediction targets.** Following prior work [5], we adopt *pass@1* as a primary correctness signal, capturing whether the model succeeds on its first attempt. Since *pass@1* is binary, it does not distinguish near-correct programs from substantially incorrect ones. We therefore use *partial\_pass@1* as a complementary, graded execution-based target, defined as the proportion of test cases passed by the first sampled program, as in [23]. This provides a useful measure of *partial correctness*.

**Evaluation metrics.** For *pass@1*, which is a binary outcome, we evaluate how well uncertainty scores *discriminate* between correct and incorrect generations using the area under the ROC curve (AUROC) [4]. For the continuous-valued *partial\_pass@1*, we assess its association with uncertainty scores using Pearson [3] and Spearman [26] correlation coefficients, capturing linear and monotonic relationships, respectively.

## 4.2 Answering RQ1 (Predictive Performance)

**pass@1 and partial\_pass@1 prediction.** Table 2 reports AUROC for *pass@1* failure prediction and Pearson  $r$ /Spearman  $\rho$  correlations with *partial\_pass@1* on *LiveCodeBench*. Across all four models, SDE and DSDE provide strong predictive signals: DSDE achieves AUROC above 0.8 in every setting, and both metrics correlate negatively with *partial\_pass@1*, indicating that higher uncertainty corresponds to lower partial correctness.

On the main closed-source LiveCodeBench evaluation, DSDE improves over SDE across all models and metrics, supporting the top-anchored design: when assessing the program shown to the user, uncertainty can be more informative when measured relative to that program’s behaviour rather than averaged uniformly across all samples. This advantage may depend on the first sample being representative; when it is not, as suggested by DeepSeek-Coder-V2 in Table 3, the symmetric SDE estimator can be more stable.

**Comparison with baselines.** We compare against three strong baselines, chosen to cover the main existing design choices in Table 1: DiffTrust, the state-of-the-art incoherence-based proxy [24]; HonestCoder, a representative confidence estimator combining embeddings, data-flow signatures, and syntactic  $n$ -grams [17]; and Semantic Entropy, the standard entropy-based uncertainty estimator over LLM-judged semantic clusters [7]. As shown in Table 2, even these competitive baselines are only weakly informative on *LiveCodeBench*. By contrast, SDE and DSDE outperform every baseline on every model and metric, suggesting that graded semantic distance captures correctness-relevant information missed by binary disagreement and marginal entropy-based uncertainty.

Table 2: Performance of SDE, DSDE, and the three baselines on *LiveCodeBench* across models ( $T = 0.6$ ). Best result per metric per row is shown in bold. AUC denotes AUROC;  $r$  and  $\rho$  are Pearson and Spearman correlations with *partial\_pass@1*, respectively. Per-difficulty breakdowns (Easy/Medium/Hard) are reported in Appendix C.1.

Model	SDE			DSDE			DiffTrust			HC			Semantic Entropy		
	AUC	$r$	$\rho$	AUC	$r$	$\rho$	AUC	$r$	$\rho$	AUC	$r$	$\rho$	AUC	$r$	$\rho$
GPT-3.5-Turbo-0125	0.827	-0.587	-0.581	<b>0.844</b>	-0.622	-0.620	0.669	-0.259	-0.267	0.646	-0.344	-0.328	0.605	-0.240	-0.237
GPT-4o-mini	0.826	-0.589	-0.584	<b>0.844</b>	-0.624	-0.624	0.534	-0.024	-0.064	0.646	-0.344	-0.328	0.607	-0.240	-0.238
Gemini-2.5-Flash-Lite	0.794	-0.494	-0.491	<b>0.808</b>	-0.532	-0.512	0.688	-0.296	-0.298	0.668	-0.301	-0.329	0.639	-0.237	-0.242
Claude-opus-4.5	0.818	-0.552	-0.450	<b>0.825</b>	-0.611	-0.461	0.606	-0.139	-0.139	0.739	-0.424	-0.350	0.687	-0.275	-0.287

## 4.3 Answering RQ2 (Generalisation)

**Across benchmarks of varying difficulty.** The first block of Table 3 evaluates SDE and DSDE on three Python benchmarks spanning entry-level function completion (MBPP), competitive programming (*LiveCodeBench*), and repository-scale tasks (BigCodeBench). Both metrics retain strong predictive performance on MBPP and *LiveCodeBench*, with AUROC above 0.75 and Spearman correlations close to  $-0.6$ .

*Beyond function-level benchmarks: BigCodeBench.* BigCodeBench is the most demanding benchmark we consider and, to our knowledge, the first repository-scale evaluation of sample-based uncertainty estimation for LLM-generated code. Its tasks include cross-file dependencies, side effects, stochastic operations, and often a range of valid outputs for the same specification. This makes exact-match execution clustering too brittle: semantically valid programs may produce different concrete outputs and be incorrectly separated.

Our formulation can accommodate this setting because it is agnostic with respect to the clustering proxy. We therefore make a single drop-in change: instead of clustering by exact output match, we use whitebox fuzzing [10] to target specification predicates and group programs by predicate satisfaction. With this adaptation, DSDE achieves AUROC 0.668 and Spearman  $\rho = -0.335$  on BigCodeBench. Although lower than on function-level benchmarks, this remains a non-trivial signal in a substantially more challenging repository-scale regime.

**Across programming languages.** On HumanEval-X [28], covering Python, Java, and C++, both metrics perform consistently across languages without language-specific tuning.

**Across sampling temperatures.** We sweep the sampling temperature  $T \in \{0.2, 0.6, 0.8\}$  using GPT-4o-mini on *LiveCodeBench*. As shown in Table 3, performance improves with temperature: lower temperatures reduce sample diversity, while higher temperatures expose richer behavioural variation for uncertainty estimation. Nevertheless, SDE and DSDE remain informative across all settings, indicating that distance-aware uncertainty benefits from, but does not depend on, high sampling diversity.

**Across model families.** Finally, we evaluate on the open-weights DeepSeek-Coder-V2 model, which achieves *pass@1* of 38.14% on *LiveCodeBench*. Both metrics retain meaningful AUROC and correlations with *partial\_pass@1*, showing that the distance-aware signal transfers beyond the closed-source models used in RQ1.

Table 3: Performance of SDE and DSDE across benchmarks, languages, sampling temperatures, and model families (GPT-4o-mini,  $T = 0.6$ , unless noted). Better of SDE/DSDE per row in AUROC in bold. Per-difficulty *LiveCodeBench* breakdowns are in Appendix C.1.

Benchmark	AUROC		Pearson $r$		Spearman $\rho$	
	SDE	DSDE	SDE	DSDE	SDE	DSDE
<i>Increased difficulty (Python benchmarks, easy to hard)</i>						
MBPP	0.751	<b>0.752</b>	-0.480	-0.434	-0.601	-0.595
LiveCodeBench	0.826	<b>0.844</b>	-0.589	-0.624	-0.584	-0.624
BigCodeBench	0.664	<b>0.668</b>	-0.281	-0.287	-0.333	-0.335
<i>Programming languages (HumanEval-X)</i>						
Python	0.751	<b>0.757</b>	-0.523	-0.521	-0.631	-0.634
Java	0.740	<b>0.745</b>	-0.509	-0.516	-0.605	-0.603
C++	0.796	<b>0.804</b>	-0.599	-0.619	-0.573	-0.587
<i>Sampling temperature (GPT-4o-mini, LCB)</i>						
$T = 0.2$	<b>0.780</b>	0.779	-0.538	-0.529	-0.524	-0.522
$T = 0.6$	0.826	<b>0.844</b>	-0.589	-0.624	-0.584	-0.624
$T = 0.8$	0.837	<b>0.853</b>	-0.612	-0.660	-0.609	-0.646
<i>Open-weights model (LCB)</i>						
DeepSeek-Coder-V2	<b>0.778</b>	0.769	-0.483	-0.469	-0.479	-0.462

#### 4.4 Answering RQ3 (Cost-effectiveness)

**Scaling  $K$  and  $N$  up to test for further gains.** To check whether allocating a larger budget improves predictive performance, we extend the sensitivity analysis on a 50-task *LiveCodeBench* subset across all four code-generation models. Sweeping  $K \in \{5, 10, 15, 20\}$  at fixed  $N = 10$  leaves DSDE AUROC within 0.024 of the default  $(K, N) = (10, 10)$  across all values; sweeping  $N$  from 10 up to 1,000 at fixed  $K = 10$  likewise produces no measurable trend (Figure 1). Both sweeps indicate that scaling  $K$  or  $N$  beyond the default  $(K, N) = (10, 10)$  yields no measurable predictive gain.

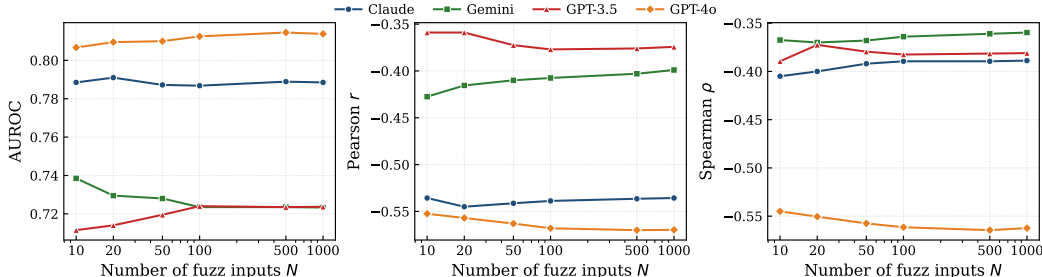


Figure 1: Sensitivity of DSDE to the number of fuzz inputs  $N$  on a 50-task *LiveCodeBench* subset, with  $K$  fixed to 10. AUROC, Pearson  $r$ , and Spearman  $\rho$  remain essentially flat across  $N \in \{10, 20, 50, 100, 500, 1000\}$  for all four code-generation models.

**Scaling  $K$  and  $N$  down to find the minimal viable configuration.** Since enlarging the budget does not help, we instead probe how far  $(K, N)$  can be reduced before the predictive signal degrades.

We sweep  $K, N \in \{3, 5, 8, 10\}$  jointly (Figure 2). The smallest configuration  $(K, N) = (3, 3)$  already yields AUROC 0.783, recovering  $\sim 93\%$  of the AUROC at  $(10, 10)$  while requiring an order-of-magnitude less sample and execution cost. Therefore,  $(3, 3)$  can be adopted as a cost-effective deployment default for budget-constrained settings.

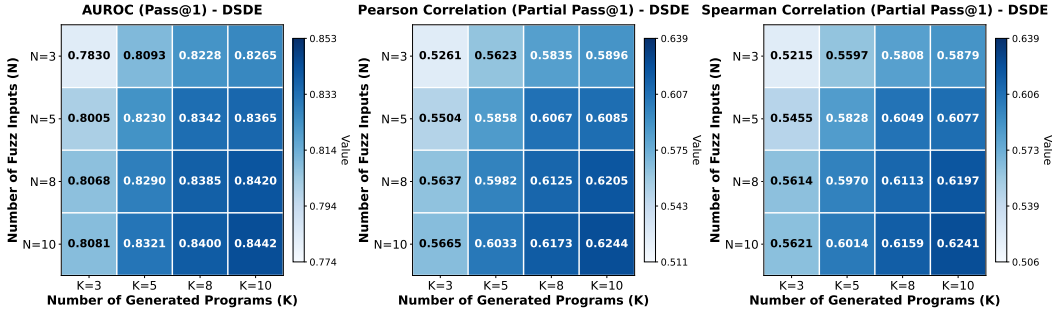


Figure 2: Joint cost-effectiveness analysis of DSDE on *LiveCodeBench* (GPT-4o-mini,  $T = 0.6$ ), varying  $K \in \{3, 5, 8, 10\}$  and  $N \in \{3, 5, 8, 10\}$ .

**Runtime against baselines.** We now compare end-to-end wall-clock cost against other uncertainty estimators. Table 4 breaks runtime into: candidate-program sampling, additional model-side computation (*Model Cost*, e.g. embeddings or LLM-as-judge calls), fuzz-input generation, program execution and metric computation. The sampling cost is shared across methods; the main differences arise from the additional model-side or execution costs required by each estimator.

At the default  $(K, N) = (10, 10)$ , our method takes on average  $\sim 5.7$  s per task, compared with  $\sim 11$  s for HonestCoder,  $\sim 13$  s for Semantic Entropy, and  $\sim 27$  s for DiffTrust. This is a  $\sim 79\%$  reduction relative to state-of-the-art DiffTrust. With the deployment default  $(K, N) = (3, 3)$ , the runtime falls further to  $\sim 2$  s per task.

Table 4: Per-task runtime breakdown on *LiveCodeBench* with GPT-4o-mini.

Method	$N$	Sampling	Model Cost	Fuzzing	Execution	Metric	Total
HonestCoder	—	$\sim 3$ s	$\sim 7$ s	—	—	$\sim 1$ s	$\sim 11$ s
Semantic Entropy	—	$\sim 3$ s	$\sim 10$ s	—	—	$< 1$ ms	$\sim 13$ s
DiffTrust	1000	$\sim 3$ s	—	$\sim 3$ s	$\sim 20$ s	$\sim 1$ s	$\sim 27$ s
Ours	10	$\sim 3$ s	—	$< 5$ ms	$\sim 2.7$ s	$< 1$ ms	$\sim 5.7$ s

The saving comes from two design choices: (i) distance-aware uncertainty metrics avoid model costs entirely (no embeddings, no LLM-as-judge); and (ii) while DiffTrust requires  $N = 1,000$  test inputs by default to satisfy the variance bounds of its Monte Carlo incoherence estimator, our metric is a deterministic pairwise aggregate over execution clusters and does not depend on a large  $N$  for statistical guarantees.

#### 4.5 Answering RQ4 (Robustness to Design Choices)

**Robustness to graded disagreement costs  $(a, b, c)$ .** The graded disagreement costs  $(a, b, c)$  are fixed to  $(1, 0.8, 0.6)$  throughout the experiments above. To quantify the gap between this fixed scheme and a per-setting tuned alternative, we additionally fit  $(a, b, c)$  via an 80:20 train-test split per model on *LiveCodeBench* at  $T = 0.6$ . As shown in Table 5, the default and learned schemes differ by less than 0.011 AUROC across all four models, indicating that the fixed weights are sufficient on *LiveCodeBench*. In our current experiments, the default setting appears to be stable and strong, but learned weights may still be useful in future settings or datasets with different failure patterns.

**Robustness under seed-free input generation (no dataset-provided test inputs).** In contrast to the seeded experiments above (where the fuzzer mutates benchmark-provided test inputs as initial seeds), we further evaluate a *seed-free* variant in which the fuzzer never reads benchmark-provided test cases, expected outputs, or reference implementations. Parameter types are inferred by a rule-based parser from the function interface, using type annotations when available and parameter names or natural-language hints from the prompt otherwise. Inputs are then sampled from generic type-level

Table 5: Robustness to distance weights  $(a, b, c)$ : fixed default  $(1.0, 0.8, 0.6)$  vs. per-setting learned weights on *LiveCodeBench* (GPT-4o-mini,  $T = 0.6$ , 80:20 train-test split per model).

Setting	$(a, b, c)$	Default	Learned	$\Delta$
Claude Opus 4.5	(0.90, 0.90, 0.25)	0.8248	0.8206	-0.0042
Gemini-2.5-Flash-Lite	(0.90, 0.90, 0.90)	0.8075	0.7974	-0.0101
GPT-3.5-Turbo	(0.97, 0.88, 0.88)	0.8442	0.8395	-0.0047
GPT-4o-mini	(1.00, 0.80, 0.80)	0.8442	0.8524	+0.0082

distributions. As shown in Table 6, the AUROC degradation is small (at most 0.087) and the predictive signal remains substantially above chance across all benchmarks, confirming that SDE and DSDE are fuzzer-agnostic.

Table 6: Robustness to fuzz-input seeds: AUROC, Pearson, and Spearman across three fuzzer seeds on *LiveCodeBench* (GPT-4o-mini,  $T = 0.6$ ).

Benchmark	SDE			DSDE		
	Seed	Seed-free	$\Delta$	Seed	Seed-free	$\Delta$
MBPP	0.751	0.712	-0.039	0.752	0.711	-0.041
LiveCodeBench	0.826	0.786	-0.040	0.844	0.787	-0.057
HumanEval-X (Python)	0.751	0.705	-0.046	0.757	0.704	-0.053
HumanEval-X (Java)	0.748	0.725	-0.023	0.745	0.731	-0.014
HumanEval-X (C++)	0.796	0.709	-0.087	0.804	0.723	-0.081

**Robustness to fuzz-input random seeds.** Here, “seed” refers to the random seed of the fuzz-input generator, not to the benchmark-provided seed inputs used to initialise fuzzing. We keep the tasks, prompts, sampled programs, and benchmark-provided initial inputs fixed, and rerun only the fuzzing step with three different random seeds. This isolates the effect of randomness in the mutation process itself. We re-run the *LiveCodeBench* pipeline on GPT-4o-mini ( $T = 0.6$ ,  $K = N = 10$ ) under three independent fuzz-input-generator seeds. As shown in Table 7, cross-seed standard deviations are at most 0.0024 on AUROC and 0.0050 on Spearman for both SDE and DSDE, indicating that the reported numbers do not depend on the choice of seed.

Table 7: Robustness to fuzz-input-generator randomness on *LiveCodeBench* (GPT-4o-mini,  $T = 0.6$ ,  $K = N = 10$ ). The random seed controlling fuzz-input mutations is varied. Results report mean  $\pm$  standard deviation over three independent fuzz-input-generator seeds.

Metric	AUROC	Pearson	Spearman
SDE	0.8238 $\pm$ 0.0011	-0.5880 $\pm$ 0.0035	-0.5831 $\pm$ 0.0022
DSDE	<b>0.8413 <math>\pm</math> 0.0005</b>	<b>-0.6249 <math>\pm</math> 0.0030</b>	<b>-0.6240 <math>\pm</math> 0.0023</b>

## 5 Limitations

Our framework inherits several limitations from its underlying assumptions. (i) *Equivalence proxy.* Effectiveness depends on the proxy exposing meaningful behavioural differences; weak fuzz inputs may yield overly coarse equivalence classes. (ii) *Fuzzing is not a correctness oracle.* Two incorrect programs may agree on all sampled inputs but diverge elsewhere, and two valid programs may disagree when the specification admits multiple acceptable behaviours, as seen on BigCodeBench. (iii) *Top-ranked reference.* When the top-ranked sample is unrepresentative of the model’s behavioural distribution, anchoring becomes unstable, consistent with our DeepSeek-Coder-V2 result where SDE slightly outperforms DSDE. (iv) *Heuristic graded distance.* The abnormal-execution costs  $(a, b, c)$  are hyperparameters with no canonical value across failure modes. Weights may need adaptation for other runtimes, languages, or benchmarks.

## 6 Conclusions

We introduced a four-axis taxonomy of sample-based uncertainty estimators (Table 1) and identified an unoccupied region: pairwise uncertainty estimation with graded semantic dissimilarity. We

instantiated this region with two estimators: SDE, a symmetric Rao quadratic entropy over execution clusters, and DSDE, a top-anchored variant measuring disagreement between alternative samples and the served output. Both improve predictive performance over sample-based baselines at lower computational cost, and remain stable across benchmarks, languages, temperatures and fuzzing settings.

## References

- [1] Yasin Abbasi-Yadkori, Ilja Kuzborskij, András György, and Csaba Szepesvari. To believe or not to believe your llm: Iterative prompting for estimating epistemic uncertainty. In *The Thirty-eighth Annual Conference on Neural Information Processing Systems*, 2024.
- [2] Jacob Austin, Augustus Odena, Maxwell I. Nye, Maarten Bosma, Henryk Michalewski, David Dohan, Ellen Jiang, Carrie J. Cai, Michael Terry, Quoc V. Le, and Charles Sutton. Program synthesis with large language models. *CoRR*, abs/2108.07732, 2021. URL <https://arxiv.org/abs/2108.07732>.
- [3] Jacob Benesty, Jingdong Chen, Yiteng Huang, and Israel Cohen. Pearson correlation coefficient. In *Noise Reduction in Speech Processing*, volume 2 of *Springer Topics in Signal Processing*, pages 1–37. Springer, Berlin, Heidelberg, 2009. ISBN 978-3-642-00296-0. doi: 10.1007/978-3-642-00296-0\_5.
- [4] Andrew P. Bradley. The use of the area under the ROC curve in the evaluation of machine learning algorithms. *Pattern Recognition*, 30(7):1145–1159, 1997. ISSN 0031-3203. doi: 10.1016/S0031-3203(96)00142-2.
- [5] Mark Chen, Jerry Tworek, Heewoo Jun, Qiming Yuan, Henrique Ponde de Oliveira Pinto, Jared Kaplan, Harri Edwards, Yuri Burda, Nicholas Joseph, Greg Brockman, et al. Evaluating large language models trained on code, 2021. URL <https://arxiv.org/abs/2107.03374>.
- [6] Vítor Mateus de Brito and Kleinner Farias. Understanding the role of large language models in software engineering: Evidence from an industry survey, 2025. URL <https://arxiv.org/abs/2512.21347>.
- [7] Sebastian Farquhar, Jannik Kossen, Lorenz Kuhn, and Yarin Gal. Detecting hallucinations in large language models using semantic entropy. *Nature*, 630(8017):625–630, 2024. doi: 10.1038/s41586-024-07421-0.
- [8] Robert Friel and Amartya Sanyal. Chainpoll: A high efficacy method for llm hallucination detection. arXiv preprint arXiv:2310.18344, 2023. URL <https://arxiv.org/abs/2310.18344>.
- [9] Cuiyun Gao, Guodong Fan, Chun Yong Chong, Shizhan Chen, Chao Liu, David Lo, Zibin Zheng, and Qing Liao. A systematic literature review of code hallucinations in llms: Characterization, mitigation methods, challenges, and future directions for reliable ai, 2025. URL <https://arxiv.org/abs/2511.00776>.
- [10] Patrice Godefroid, Michael Y Levin, David A Molnar, et al. Automated whitebox fuzz testing. In *Ndss*, volume 8, pages 151–166, 2008.
- [11] Daya Guo, Dejian Yang, Haowei Zhang, Junxiao Song, Peiyi Wang, Qihao Zhu, Runxin Xu, Ruoyu Zhang, Shirong Ma, Xiao Bi, Xiaokang Zhang, Xingkai Yu, Yu Wu, Z. F. Wu, Zhibin Gou, Zhihong Shao, Zhuoshu Li, Ziyi Gao, Aixin Liu, Bing Xue, Bingxuan Wang, Bochao Wu, Bei Feng, Chengda Lu, Chenggang Zhao, Chengqi Deng, Chong Ruan, Damai Dai, Deli Chen, Dongjie Ji, Erhang Li, Fangyun Lin, Fucong Dai, Fuli Luo, Guangbo Hao, Guanting Chen, Guowei Li, H. Zhang, Hanwei Xu, Honghui Ding, Huazuo Gao, Hui Qu, Hui Li, Jianzhong Guo, Jiashi Li, Jingchang Chen, Jingyang Yuan, Jinhao Tu, Junjie Qiu, Junlong Li, J. L. Cai, Jiaqi Ni, Jian Liang, Jin Chen, Kai Dong, Kai Hu, Kaichao You, Kaige Gao, Kang Guan, Kexin Huang, Kuai Yu, Lean Wang, Lecong Zhang, Liang Zhao, Litong Wang, Liyue Zhang, Lei Xu, Leyi Xia, Mingchuan Zhang, Minghua Zhang, Minghui Tang, Mingxu Zhou, Meng Li, Miaojun Wang, Mingming Li, Ning Tian, Panpan Huang, Peng Zhang, Qiancheng Wang, Qinyu Chen, Qiusi Du, Ruiqi Ge, Ruisong Zhang, Ruizhe Pan, Runji Wang, R. J. Chen, R. L. Jin, Ruyi

- Chen, Shanghao Lu, Shangyan Zhou, Shanhuang Chen, Shengfeng Ye, Shiyu Wang, Shuiping Yu, Shunfeng Zhou, Shuting Pan, S. S. Li, Shuang Zhou, Shaoqing Wu, Tao Yun, Tian Pei, Tianyu Sun, T. Wang, Wangding Zeng, Wen Liu, Wenfeng Liang, Wenjun Gao, Wenqin Yu, Wentao Zhang, W. L. Xiao, Wei An, Xiaodong Liu, Xiaohan Wang, Xiaokang Chen, Xiaotao Nie, Xin Cheng, Xin Liu, Xin Xie, Xingchao Liu, Xinyu Yang, Xinyuan Li, Xuecheng Su, Xuheng Lin, X. Q. Li, Xiangyue Jin, Xiaojin Shen, Xiaosha Chen, Xiaowen Sun, Xiaoxiang Wang, Xinnan Song, Xinyi Zhou, Xianzu Wang, Xinxia Shan, Y. K. Li, Y. Q. Wang, Y. X. Wei, Yang Zhang, Yanhong Xu, Yao Li, Yao Zhao, Yaofeng Sun, Yaohui Wang, Yi Yu, Yichao Zhang, Yifan Shi, Yiliang Xiong, Ying He, Yishi Piao, Yisong Wang, Yixuan Tan, Yiyang Ma, Yiyuan Liu, Yongqiang Guo, Yuan Ou, Yuduan Wang, Yue Gong, Yuheng Zou, Yujia He, Yunfan Xiong, Yuxiang Luo, Yuxiang You, Yuxuan Liu, Yuyang Zhou, Y. X. Zhu, Yanping Huang, Yaohui Li, Yi Zheng, Yuchen Zhu, Yunxian Ma, Ying Tang, Yukun Zha, Yuting Yan, Z. Z. Ren, Zehui Ren, Zhangli Sha, Zhe Fu, Zhean Xu, Zhenda Xie, Zhengyan Zhang, Zhewen Hao, Zhicheng Ma, Zhigang Yan, Zhiyu Wu, Zihui Gu, Zijia Zhu, Zijun Liu, Zilin Li, Ziwei Xie, Ziyang Song, Zizheng Pan, Zhen Huang, Zhipeng Xu, Zhongyu Zhang, and Zhen Zhang. Deepseek-r1 incentivizes reasoning in large language models through reinforcement learning. *Nature*, 645(8081):633–638, 2025.
- [12] James A. Hanley and Barbara J. McNeil. The meaning and use of the area under a receiver operating characteristic (roc) curve. *Radiology*, 143(1):29–36, 1982.
- [13] Dan Hendrycks, Steven Basart, Saurav Kadavath, Mantas Mazeika, Akul Arora, Ethan Guo, Collin Burns, Samir Puranik, Horace He, Dawn Song, and Jacob Steinhardt. Measuring coding challenge competence with APPS, 2021. URL <https://arxiv.org/abs/2105.09938>.
- [14] Yuheng Huang, Jiayang Song, Zhijie Wang, Shengming Zhao, Huaming Chen, Felix Juefei-Xu, and Lei Ma. Look before you leap: An exploratory study of uncertainty analysis for large language models. *IEEE Transactions on Software Engineering*, 51(2):413–429, 2025. doi: 10.1109/TSE.2024.3519464.
- [15] Naman Jain, King Han, Alex Gu, Wen-Ding Li, Fanjia Yan, Tianjun Zhang, Sida Wang, Armando Solar-Lezama, Koushik Sen, and Ion Stoica. Livecodebench: Holistic and contamination free evaluation of large language models for code. In *The Thirteenth International Conference on Learning Representations, ICLR 2025, Singapore, April 24-28, 2025*. OpenReview.net, 2025. URL <https://openreview.net/forum?id=chfJJYC3iL>.
- [16] Lorenz Kuhn, Yarin Gal, and Sebastian Farquhar. Semantic uncertainty: Linguistic invariances for uncertainty estimation in natural language generation. In *The Eleventh International Conference on Learning Representations, ICLR 2023, Kigali, Rwanda, May 1-5, 2023*. OpenReview.net, 2023. URL <https://openreview.net/forum?id=VD-AYtP0dve>.
- [17] Jingxuan Li, Yuxin Zhu, Yiming Li, Guoping Li, and Zhi Jin. Showing llm-generated code selectively based on confidence of llms. arXiv preprint arXiv:2410.03234, 2024. URL <https://arxiv.org/abs/2410.03234>.
- [18] Zhen Lin, Shubhendu Trivedi, and Jimeng Sun. Generating with confidence: Uncertainty quantification for black-box large language models. *arXiv preprint arXiv:2305.19187*, 2023.
- [19] Jiawei Liu, Chunqiu Steven Xia, Yuyao Wang, and Lingming Zhang. Is your code generated by chatgpt really correct? rigorous evaluation of large language models for code generation, 2023. URL <https://arxiv.org/abs/2305.01210>.
- [20] Potsawee Manakul, Ankit Liusie, and Mark J. F. Gales. Selfcheckgpt: Zero-resource black-box hallucination detection for generative large language models. arXiv preprint arXiv:2303.08896, 2023. URL <https://arxiv.org/abs/2303.08896>.
- [21] Nhan Nguyen and Sarah Nadi. An empirical evaluation of github copilot’s code suggestions. In *Proceedings of the 19th International Conference on Mining Software Repositories (MSR)*, pages 1–5, 2022. doi: 10.1145/3524842.3528470.
- [22] Rodrigo Pato Nogueira, Marco Vieira, and João R. Campos. Beyond functional correctness: An empirical evaluation of large language models for text-to-code generation. In *Proceedings of the IEEE International Symposium on Software Reliability Engineering (ISSRE)*, pages 264–275, 2025. doi: 10.1109/ISSRE66568.2025.00036.

- [23] Arindam Sharma and Cristina David. Assessing correctness in LLM-based code generation via uncertainty estimation, 2025. URL <https://arxiv.org/abs/2502.11620>.
- [24] Thomas Valentin, Ardi Madadi, Gaetano Sapia, and Marcel Böhme. Incoherence as oracle-less measure of error in LLM-based code generation. In *Proceedings of the 40th AAAI Conference on Artificial Intelligence (AAAI)*, 2026. Accepted for publication.
- [25] Xuezhi Wang, Jason Wei, Dale Schuurmans, Quoc V. Le, Ed H. Chi, Sharan Narang, Aakanksha Chowdhery, and Denny Zhou. Self-consistency improves chain of thought reasoning in language models. In *The Eleventh International Conference on Learning Representations, ICLR 2023, Kigali, Rwanda, May 1-5, 2023*. OpenReview.net, 2023. URL <https://openreview.net/forum?id=1PL1NIMMrw>.
- [26] Clark Wissler. The spearman correlation formula. *Science*, 22(558):309–311, 1905. doi: 10.1126/science.22.558.309.
- [27] Sangyeop Yeo, Yu-Seung Ma, Sang Cheol Kim, Hyungkook Jun, and Taeho Kim. Framework for evaluating code generation ability of large language models. *ETRI Journal*, 46(1):106–117, 2024. doi: 10.4218/etrij.2023-0357.
- [28] Qinkai Zheng, Xiao Xia, Xu Zou, Yuxiao Dong, Shan Wang, Yufei Xue, Lei Shen, Zihan Wang, Andi Wang, Yang Li, Teng Su, Zhilin Yang, and Jie Tang. Codegeex: A pre-trained model for code generation with multilingual benchmarking on humaneval-x. In Ambuj K. Singh, Yizhou Sun, Leman Akoglu, Dimitrios Gunopulos, Xifeng Yan, Ravi Kumar, Fatma Ozcan, and Jieping Ye, editors, *Proceedings of the 29th ACM SIGKDD Conference on Knowledge Discovery and Data Mining, KDD 2023, Long Beach, CA, USA, August 6-10, 2023*, pages 5673–5684. ACM, 2023. doi: 10.1145/3580305.3599790. URL <https://doi.org/10.1145/3580305.3599790>.
- [29] Terry Yue Zhuo, Minh Chien Vu, Jenny Chim, Han Hu, Wenhao Yu, Ratnadira Widyasari, Imam Nur Bani Yusuf, Haolan Zhan, Junda He, Indraneil Paul, Simon Brunner, Chen Gong, James Hoang, Armel Randy Zebaze, Xiaoheng Hong, Wen-Ding Li, Jean Kaddour, Ming Xu, Zhihan Zhang, Prateek Yadav, and et al. Bigcodebench: Benchmarking code generation with diverse function calls and complex instructions. In *The Thirteenth International Conference on Learning Representations, ICLR 2025, Singapore, April 24-28, 2025*. OpenReview.net, 2025. URL <https://openreview.net/forum?id=YrycTj11L0>.

## A Detailed Input-Quality Diagnostics

The reliability of SDE and DSDE ultimately depends on whether the generated test inputs  $\mathcal{I}$  produce useful behavioural signal on the sampled programs. This appendix reports four diagnostics that characterise this signal, computed per task over  $\mathcal{I} = \{x_1, \dots, x_{10}\}$  and the candidate set  $\mathcal{C}$ , and averaged across tasks. We organise the diagnostics into two groups: (i) input-side validity metrics that measure how well  $\mathcal{I}$  is constructed; (ii) coverage metrics that measure how thoroughly  $\mathcal{I}$  exercises the candidate code.

### Input validity metrics

**ValidExecRate** is the fraction of inputs on which at least one candidate program returns a non-crash output. An input on which every candidate crashes carries no behavioural signal and cannot contribute to clustering:

$$\text{ValidExecRate} = \frac{|\{x_j \in \mathcal{I} : \exists c \in \mathcal{C}, c(x_j) \text{ is non-crash}\}|}{|\mathcal{I}|}. \quad (5)$$

**UniqueInputRate** is the fraction of inputs that remain distinct after canonical normalisation. A value below one indicates that the fuzzer has produced redundant or equivalent inputs within the same task:

$$\text{UniqueInputRate} = \frac{|\text{unique}(\{\text{normalize}(x_j) : x_j \in \mathcal{I}\})|}{|\mathcal{I}|}. \quad (6)$$

**CrashPollutionRate** is the fraction of all candidate-by-input execution cells that crash. A high rate indicates that many cells contribute no meaningful behavioural signal and therefore add noise to clustering:

$$\text{CrashPollutionRate} = \frac{|\{(c, x_j) \in \mathcal{C} \times \mathcal{I} : c(x_j) \text{ crashes}\}|}{|\mathcal{C}| \cdot |\mathcal{I}|}. \quad (7)$$

### Code-coverage metrics

**LineCoverage** and **BranchCoverage** measure the fraction of executable lines and branches in the candidate programs that are exercised by  $\mathcal{I}$ . For each candidate  $c \in \mathcal{C}$ , let  $L(c)$  and  $L_{\text{cov}}(c)$  denote the total and covered executable lines when  $c$  is executed on  $\mathcal{I}$ , and let  $B(c)$  and  $B_{\text{cov}}(c)$  denote the analogous quantities for branches. The micro-averaged coverages are

$$\text{LineCoverage} = \frac{\sum_{c \in \mathcal{C}} L_{\text{cov}}(c)}{\sum_{c \in \mathcal{C}} L(c)}, \quad \text{BranchCoverage} = \frac{\sum_{c \in \mathcal{C}} B_{\text{cov}}(c)}{\sum_{c \in \mathcal{C}} B(c)}. \quad (8)$$

Together they bound how much of each candidate’s behaviour is observable through the fuzz suite.

Table 8: Input-quality diagnostics on *LiveCodeBench* at  $T = 0.6$ . Per task we use the first  $N = 10$  available inputs; tasks with no available inputs are excluded. Each metric is averaged over the remaining tasks. LineCov and BranchCov are micro-averaged.

Model	ValidExec	Unique	Crash	LineCov	BranchCov
GPT-3.5-Turbo	0.901	0.948	0.209	0.937	0.888
GPT-4o-mini	0.898	0.948	0.213	0.937	0.889
Gemini-2.5-Flash-Lite	0.851	0.951	0.269	0.919	0.874
Claude-opus-4.5	0.863	0.950	0.201	0.917	0.879

### Results.

Table 8 reports the diagnostics on *LiveCodeBench* at  $T = 0.6$ . UniqueInputRate is approximately 0.95 across all four models, and ValidExecRate stays above 0.85, indicating that the fuzzer rarely produces redundant inputs and that most inputs successfully exercise at least one candidate program. LineCoverage exceeds 0.91 and BranchCoverage exceeds 0.87 on every model, indicating that the fuzz suite reaches most code paths in each candidate. The input pool therefore remains diverse, mostly

executable, and largely covering across all four models. CrashPollutionRate sits around 0.20–0.27, indicating that roughly one in five execution cells contributes no behavioural signal; reducing this rate (e.g. via type-aware input constraints or LLM-guided fuzzers) is a direct lever for strengthening the upstream signal that SDE and DSDE consume.

## B End-to-End Evaluation Pipeline

Figure 3 summarises the end-to-end evaluation pipeline used in this paper. Candidate programs are first sampled from the code generation model; type-aware mutations then produce a shared set of inputs; each candidate is executed on this input set to obtain an execution signature; programs with identical signatures are clustered; and finally the distance-aware uncertainty metrics SDE and DSDE are computed from the resulting cluster distribution.

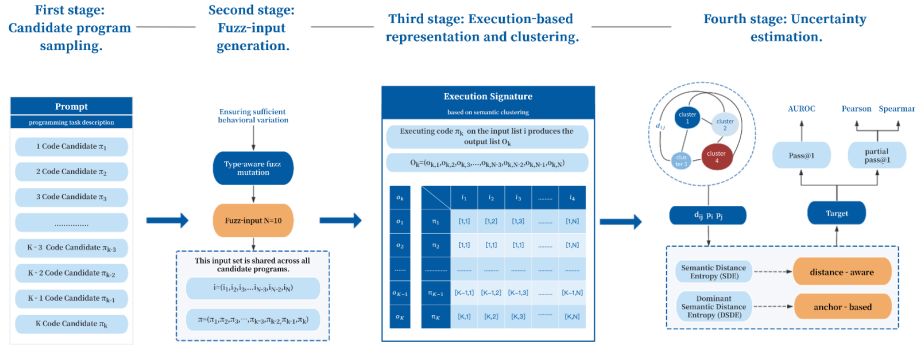


Figure 3: End-to-end evaluation pipeline for execution-based uncertainty estimation in code generation.

## C Extended Experimental Results

This appendix presents additional experimental analyses that complement the main evaluation in Section 4. Unless stated otherwise, all settings follow the protocol used in the main paper:  $K = 10$  sampled programs and  $N = 10$  test inputs per task, with execution timeout 0.2s and sampling temperature  $T = 0.6$ .

### C.1 Extended Per-Difficulty Tables

Table 9 and Table 10 correspond directly to the AUROC and correlation tables in the main paper, evaluated on four closed-source code-generation models — GPT-3.5-Turbo-0125, GPT-4o-mini, Gemini-2.5-Flash-Lite, and Claude-opus-4.5 — with results for an additional open-source model (DeepSeek-Coder-V2) reported in Section 4.3. We compare our two distance-aware uncertainty metrics, SDE and DSDE, against three sample-based uncertainty baselines: DiffTrust [24], an incoherence-based behavioural-disagreement metric for code generation; HonestCoder [17], which combines semantic embeddings and dataflow features with syntactic n-gram features over sampled programs; and Semantic Entropy [7], which clusters programs based on binary semantic-equivalence judgments from an LLM judge and computes Shannon entropy over the resulting clusters.

**Discussion of the Claude-Easy outlier.** On the LCB Easy split for Claude-opus-4.5 the AUROC drops markedly relative to the other splits. This appears to be driven by extreme class imbalance: Claude achieves a pass@1 success rate of 95.34% on this subset, leaving very few failure instances. AUROC is equivalent to the Wilcoxon rank-sum statistic [12], whose standard error grows rapidly as the minority class shrinks, so small changes in the ranking of a handful of failures produce disproportionate fluctuations in the reported value.

Table 9: AUROC for pass@1 failure prediction across task difficulty levels and models ( $T = 0.6$ ).

	SDE	DSDE	DiffTrust	HonestCoder	Semantic Entropy
<b>GPT-3.5-Turbo-0125</b>					
LiveCodeBench All	0.827	<b>0.844</b>	0.669	0.646	0.605
LiveCodeBench Easy	0.786	<b>0.801</b>	0.577	0.645	0.592
LiveCodeBench Medium	0.718	<b>0.753</b>	0.610	0.576	0.548
LiveCodeBench Hard	0.806	<b>0.831</b>	0.568	0.570	0.550
<b>GPT-4o-mini</b>					
LiveCodeBench All	0.826	<b>0.844</b>	0.534	0.646	0.607
LiveCodeBench Easy	0.785	<b>0.796</b>	0.565	0.645	0.594
LiveCodeBench Medium	0.712	<b>0.752</b>	0.504	0.576	0.548
LiveCodeBench Hard	0.801	<b>0.829</b>	0.523	0.570	0.553
<b>Gemini-2.5-Flash-Lite</b>					
LiveCodeBench All	0.794	<b>0.808</b>	0.688	0.668	0.639
LiveCodeBench Easy	<b>0.735</b>	0.730	0.671	0.566	0.470
LiveCodeBench Medium	0.742	<b>0.762</b>	0.686	0.635	0.597
LiveCodeBench Hard	0.705	<b>0.737</b>	0.523	0.590	0.645
<b>Claude-opus-4.5</b>					
LiveCodeBench All	0.818	<b>0.825</b>	0.606	0.739	0.687
LiveCodeBench Easy	<b>0.483</b>	0.482	0.473	0.423	0.452
LiveCodeBench Medium	0.723	<b>0.733</b>	0.556	0.605	0.572
LiveCodeBench Hard	0.815	<b>0.839</b>	0.507	0.735	0.638

## C.2 Sensitivity to Distance Weights

The crash-aware distance weights  $(a, b, c)$  are fixed to  $(1, 0.8, 0.6)$  throughout the main paper. To quantify the gap between this fixed scheme and a per-setting tuned alternative, we additionally consider learning  $(a, b, c)$  via an 80:20 train–test split: the weights are fitted on the training set and the resulting AUROC is measured on the held-out test set.

The default and learned schemes differ by less than 0.011 in AUROC across all settings. On *LiveCodeBench*, only a small subset of inputs (consistently below 3 out of 10) result in abnormal execution and therefore depend on  $(a, b, c)$ , which explains the small gap. In domains where abnormal executions are more frequent, learning the weights is expected to become more beneficial; for the regimes considered here, the fixed weighting scheme is sufficient.

## C.3 Benchmark Details

*LiveCodeBench* (LCB) is our primary benchmark, containing 1,055 programming tasks stratified into Easy, Medium, and Hard difficulty levels with a relatively balanced distribution. *MBPP* contains 257 entry-level Python function-completion problems. *HumanEval-X* comprises 164 hand-written problems parallel-translated into Python, Java, and C++, and is used to test cross-language transfer. *BigCodeBench* consists of 1,140 repository-scale tasks featuring cross-file dependencies, multiple interacting components, and complex control flow. Together these benchmarks span a wide range of task difficulty (from entry-level to repository-scale), programming languages (Python, Java, C++), and problem styles (function completion, competitive programming, and realistic library usage).

## C.4 Abstention Policy for Practical Deployment

To support practical use of uncertainty estimates, we introduce a simple abstention policy that determines whether to accept or reject the model’s top-ranked generated solution. The policy requires no additional models or supervision; instead, it operationalises our distance-aware uncertainty metrics as an actionable decision rule.

Table 10: Correlation with partial\_pass@1 across task difficulty levels and models ( $T = 0.6$ ). Left block: Pearson  $r$ . Right block: Spearman  $\rho$ .

	Pearson $r$					Spearman $\rho$				
	SDE	DSDE	DiffTrust	HC	Semantic Entropy	SDE	DSDE	DiffTrust	HC	Semantic Entropy
<b>GPT-3.5-Turbo-0125</b>										
LiveCodeBench All	-0.587	<b>-0.622</b>	-0.259	-0.344	-0.240	-0.581	<b>-0.620</b>	-0.267	-0.328	-0.237
LiveCodeBench Easy	-0.588	<b>-0.645</b>	-0.184	-0.259	-0.169	-0.549	<b>-0.581</b>	-0.145	-0.256	-0.176
LiveCodeBench Medium	-0.412	<b>-0.467</b>	-0.153	-0.185	-0.112	-0.426	<b>-0.474</b>	-0.144	-0.179	-0.105
LiveCodeBench Hard	-0.474	<b>-0.516</b>	-0.063	-0.205	-0.144	-0.429	<b>-0.492</b>	-0.044	-0.162	-0.121
<b>GPT-4o-mini</b>										
LiveCodeBench All	-0.589	<b>-0.624</b>	-0.024	-0.344	-0.240	-0.584	<b>-0.624</b>	-0.064	-0.328	-0.238
LiveCodeBench Easy	-0.590	<b>-0.644</b>	-0.180	-0.259	-0.170	-0.547	<b>-0.571</b>	-0.143	-0.255	-0.176
LiveCodeBench Medium	-0.416	<b>-0.474</b>	0.013	-0.185	-0.110	-0.433	<b>-0.488</b>	-0.033	-0.179	-0.106
LiveCodeBench Hard	-0.470	<b>-0.515</b>	-0.018	-0.205	-0.142	-0.426	<b>-0.485</b>	-0.059	-0.162	-0.123
<b>Gemini-2.5-Flash-Lite</b>										
LiveCodeBench All	-0.494	<b>-0.532</b>	-0.296	-0.301	-0.237	-0.491	<b>-0.512</b>	-0.298	-0.329	-0.242
LiveCodeBench Easy	-0.414	<b>-0.449</b>	-0.307	-0.106	-0.005	<b>-0.314</b>	-0.308	-0.215	-0.134	-0.033
LiveCodeBench Medium	-0.446	<b>-0.499</b>	-0.346	-0.249	-0.179	-0.414	<b>-0.443</b>	-0.309	-0.275	-0.178
LiveCodeBench Hard	-0.307	<b>-0.370</b>	0.025	-0.221	-0.237	-0.308	<b>-0.365</b>	0.031	-0.184	-0.235
<b>Claude-opus-4.5</b>										
LiveCodeBench All	-0.552	<b>-0.611</b>	-0.139	-0.424	-0.275	-0.450	<b>-0.461</b>	-0.139	-0.350	-0.287
LiveCodeBench Easy	0.005	0.026	-0.056	<b>0.071</b>	0.057	0.024	0.025	0.024	<b>0.052</b>	0.048
LiveCodeBench Medium	-0.406	<b>-0.492</b>	-0.082	-0.177	-0.099	-0.253	<b>-0.265</b>	-0.059	-0.143	-0.107
LiveCodeBench Hard	-0.548	<b>-0.635</b>	0.008	-0.446	-0.252	-0.531	<b>-0.580</b>	-0.003	-0.414	-0.273

Table 11: Fixed default weights (1.0, 0.8, 0.6) vs. per-setting learned weights.

Setting	( $a, b, c$ )	Default	Learned	$\Delta$	Abnormal (/10)
<i>Across models (fixed <math>T = 0.6</math>)</i>					
Claude Opus 4.5	(0.90, 0.90, 0.25)	0.8248	0.8206	-0.0042	2.01
Gemini-2.5-Flash-Lite	(0.90, 0.90, 0.90)	0.8075	0.7974	-0.0101	2.69
GPT-3.5-Turbo	(0.97, 0.88, 0.88)	0.8442	0.8395	-0.0047	2.09
GPT-4o-mini	(1.00, 0.80, 0.80)	0.8442	0.8524	+0.0082	2.13
<i>Across temperatures (fixed GPT-4o-mini)</i>					
GPT-4o-mini ( $T = 0.2$ )	(0.51, 0.41, 0.31)	0.7789	0.7743	-0.0045	2.69
GPT-4o-mini ( $T = 0.6$ )	(1.00, 0.80, 0.80)	0.8442	0.8524	+0.0082	2.13
GPT-4o-mini ( $T = 0.8$ )	(0.60, 0.60, 0.60)	0.8530	0.8446	-0.0084	1.82

Formally, given a programming task  $\pi$  and its associated uncertainty score  $U(\pi)$ , the abstention decision is defined as

$$\delta(\pi) = \begin{cases} 1, & U(\pi) \leq \tau \quad (\text{accept}) \\ 0, & U(\pi) > \tau \quad (\text{abstain}), \end{cases}$$

where  $\tau$  is a decision threshold selected via cross-validation on training data and evaluated on held-out validation folds.

Table 13 reports abstention performance for GPT-4o-mini under different operating constraints. In *safety-oriented* settings, we impose an upper bound on the false positive rate (FPR), defined as the fraction of incorrect solutions that are accepted. For each constraint,  $\tau$  is chosen to maximise accuracy under strict correctness (Pass@1 = 1). Under a highly conservative constraint (FPR  $\leq 5\%$ ), both SDE and DSDE achieve strong and comparable performance. Under a more balanced setting (FPR  $\leq 20\%$ ), DSDE yields a consistent accuracy improvement over SDE.

Table 12: Statistics of the four benchmarks used in this paper.

Benchmark	#Tasks	Languages	Task style	Difficulty
LiveCodeBench [15]	1,055	Python	Competitive programming	Easy / Medium / Hard
MBPP [2]	257	Python	Function completion	Entry-level
HumanEval-X [28]	164	Python, Java, C++	Function completion	Mixed
BigCodeBench [29]	1,140	Python	Repository-scale, library usage	Hard

Table 13: Abstention policy performance under strict correctness ( $\text{Pass}@1 = 1.0$ ) on *LiveCodeBench* using GPT-4o-mini ( $T = 0.6$ ). Results are shown under two representative operating points: *Strict Safety* and *Balanced*. Accuracy is maximised subject to the corresponding FPR constraint. Values are reported as mean  $\pm$  standard deviation over 5-fold cross-validation.

Metric	Constraint	Accuracy	FPR
SDE	FPR $\leq 5\%$	0.745 $\pm$ 0.095	0.064 $\pm$ 0.028
DSDE	FPR $\leq 5\%$	0.745 $\pm$ 0.095	0.064 $\pm$ 0.028
SDE	FPR $\leq 20\%$	0.734 $\pm$ 0.088	0.069 $\pm$ 0.028
DSDE	FPR $\leq 20\%$	<b>0.750 <math>\pm</math> 0.095</b>	0.068 $\pm$ 0.028

### C.5 Execution Timeout

Performance is robust to the choice of per-input execution timeout (Table 14). Across all settings, the proportion of *LiveCodeBench* problems that triggered at least one timeout error is below 2%, indicating that the timeout has only a minor effect on abnormal-termination rates.

Table 14: Effect of the per-input execution timeout on SDE and DSDE (GPT-4o-mini,  $T = 0.6$ ).

Timeout (s)	AUROC			Pearson $r$			Spearman $\rho$		
	SE	SDE	DSDE	SE	SDE	DSDE	SE	SDE	DSDE
0.1	0.802	0.804	0.819	-0.505	-0.540	-0.575	-0.493	-0.534	-0.573
0.2	0.824	0.826	0.844	-0.543	-0.589	-0.624	-0.524	-0.584	-0.624
0.3	0.798	0.808	0.821	-0.499	-0.550	-0.583	-0.486	-0.545	-0.580

## D Notation

Table 15 lists every symbol used in the paper. Where the pipeline (§3) and metrics (§2) sections use different surface forms for the same object, both forms are shown joined by ‘ $\equiv$ ’.

Table 15: Notation summary. Defaults from §4.1 are in parentheses.

Symbol	Description
<i>(i) Task and model</i>	
$d$	Natural-language task description
$\text{Coder}(\cdot)$	Code-generation model
$p(\pi   d)$	Conditional distribution over programs given $d$
<i>(ii) Candidate programs</i>	
$K$	Number of candidates per task ( $K=10$ )
$\pi, \pi_k, \pi_1$	Generic / $k$ -th sampled / top-ranked candidate
$\boldsymbol{\pi} \equiv \Pi$	Candidate set $\{\pi_1, \dots, \pi_K\}$
<i>(iii) Test inputs and execution</i>	
$N$	Number of test inputs per task ( $N=10$ )
$i_\ell \equiv x_\ell$	The $\ell$ -th test input, $\ell \in \{1, \dots, N\}$
$\mathbf{i} \equiv \mathcal{I}$	Input set $(i_1, \dots, i_N)$ , shared across candidates
$\pi(i_\ell) \equiv o_\ell(\pi)$	Outcome of $\pi$ on $i_\ell$ : a normal value or labelled error
$\mathbf{o}_k \equiv \sigma_{\mathcal{I}}(\pi_k)$	Execution signature $(o_1(\pi_k), \dots, o_N(\pi_k))$
<i>(iv) Behaviour clusters</i>	
$M$	Number of clusters
$C_i,  C_i $	The $i$ -th cluster and its size
$C(\pi)$	Cluster containing program $\pi$
$p_i$	Empirical cluster probability $ C_i /K, \sum_i p_i=1$
$c^*$	Index of cluster containing $\pi_1$ , i.e. $C_{c^*} = C(\pi_1)$
<i>(v) Distances and weights</i>	
$\delta(\cdot, \cdot)$	Per-input outcome dissimilarity (Eq. (2)), $\delta \in [0, 1]$
$d_{ij}$	Cluster-level distance (Eq. (1)); symmetric, $d_{ii}=0$
$a$	Cost when exactly one outcome is abnormal ( $a=1$ )
$b$	Cost when both outcomes abnormal, different errors ( $b=0.8$ )
$c$	Cost when both outcomes abnormal, same error ( $c=0.6$ )
<i>(vi) Uncertainty metrics</i>	
SDE	Semantic Distance Entropy (Eq. (3))
DSDE	Dominant SDE, anchored at $C_{c^*}$ (Eq. (4))
$U(\pi)$	Generic uncertainty score (e.g., SDE or DSDE) used in abstention
<i>(vii) Experimental settings and targets</i>	
$T$	Sampling temperature ( $T=0.6$ )
$\tau$	Decision threshold of the abstention policy
FPR	False positive rate (incorrect solutions accepted)
pass@1	Binary: $\pi_1$ passes all reference tests
partial_pass@1	Fraction of reference tests passed by $\pi_1$ , in $[0, 1]$
AUROC	Area under ROC for predicting pass@1 failure
$r, \rho$	Pearson and Spearman correlations with partial_pass@1

## E Concrete Case Study Examples

This appendix provides full task descriptions and representative cluster implementations for the two case studies. Each task is sampled  $K = 10$  times; programs sharing identical execution outcomes on the shared test inputs are grouped into a single execution-behaviour cluster. The cluster membership for all four tasks is summarised in Table 16. To complement the results in RQ1, we present two representative case studies that explicitly isolate the effect of semantic distance between execution clusters. The first case study focuses on *binary correctness* (pass@1), while the second examines *partial correctness* (partial\_pass@1). In both cases, the tasks induce the same number of execution clusters (i.e., the same count of distinct behaviours); differences in correctness therefore arise solely from variation in the *semantic distance* between clusters rather than from the number of observed behaviours.

Table 16: Execution-behaviour cluster membership and cluster probabilities for the case-study tasks.

Task ID	Cluster	Cluster prob.	Member program indices
<b>Case A: Binary correctness distinction</b>			
3367	$C_0$	0.800 (8/10)	[0, 1, 2, 3, 4, 5, 6, 7]
3367	$C_1$	0.200 (2/10)	[8, 9]
abc332_b	$C_0$	0.200 (2/10)	[0, 3]
abc332_b	$C_1$	0.800 (8/10)	[1, 2, 4, 5, 6, 7, 8, 9]
<b>Case B: Partial correctness under identical pass@1</b>			
abc326_b	$C_0$	0.400 (4/10)	[0, 4, 5, 7]
abc326_b	$C_1$	0.600 (6/10)	[1, 2, 3, 6, 8, 9]
3163	$C_0$	0.400 (4/10)	[0, 1, 3, 8]
3163	$C_1$	0.600 (6/10)	[2, 4, 5, 6, 7, 9]

### E.1 Case A: Binary Correctness Distinction

Case A contrasts two LiveCodeBench tasks whose execution-behaviour cluster *structures* are identical (in both tasks the 10 sampled programs split into two clusters of size 8 and 2), yet whose binary correctness outcomes differ. The contrast isolates the contribution of inter-cluster semantic distance: dispersion-based statistics cannot distinguish the two cases, but the distance-aware metrics can.

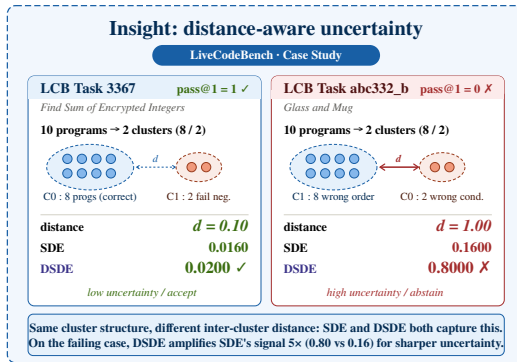


Figure 4: Case A: two LiveCodeBench tasks with identical execution-behaviour cluster structures but different inter-cluster semantic distances and binary correctness outcomes.

**Case A: Semantic Distance Explains Binary Correctness (pass@1).** Table 17 compares two tasks with identical cluster structure ( $M = 2$ , one cluster contains 2 programs, and the other 8 programs) but different binary outcomes. One task consistently produces correct executions (pass@1 = 1), while the other fails (pass@1 = 0). Importantly, both tasks exhibit the same dispersion over execution clusters, ruling out dispersion-based explanations.

Table 17: Case A: Metric-level comparison illustrating the binary correctness distinction. Task 1 (3367, pass@1 = 1) and Task 2 (abc332\_b, pass@1 = 0) induce an identical  $M = 2$  cluster structure with sizes 8 and 2, but exhibit very different inter-cluster distances.

Metric	Task 1 (Low-Distance)	Task 2 (High-Distance)	Diff.
Pass@1	1	0	-
partial_pass@1	1.0000	0.0000	<b>1.0000</b>
Clusters	2 (8/2)	2 (8/2)	<b>0</b>
Distance	0.10	1.00	<b>0.90</b>
SDE	0.0160	0.1600	<b>0.1440</b>
DSDE	0.0200	0.8000	<b>0.7800</b>

Although the two tasks induce identical cluster structures, they differ substantially in the semantic distance between clusters. For the correct task (task 1), the distance between the two clusters is small (e.g.,  $d_{01} = 0.10$ ), indicating highly similar execution outcomes. In contrast, the incorrect task (task 2) exhibits a much larger inter-cluster distance (e.g.,  $d_{01} = 1.00$ ), reflecting severe semantic divergence. This difference in cluster distance directly explains the observed binary correctness gap and is captured by distance-aware uncertainty metrics such as SDE and DSDE.

### E.1.1 Problem 3367: Find the Sum of Encrypted Integers

**Problem statement.** Given an integer array `nums`, define `encrypt(x)` as replacing every digit in `x` with the largest digit in `x`. Return the sum of encrypted elements. For example, `encrypt(523) = 555` and `encrypt(213) = 333`.

**Cluster structure.** Two clusters with probabilities  $p_0 = 0.80$  (8 samples) and  $p_1 = 0.20$  (2 samples). Cluster  $C_0$  passes all test cases; cluster  $C_1$  fails on negative-number inputs with a `ValueError`.

Cluster $C_0$ — Correct implementation (8 samples)	Key characteristic
<pre> 1 class Solution: 2     def sumOfEncryptedInt(self, nums: List[int]) -&gt; int: 3         total_sum = 0 4         for num in nums: 5             max_digit = max(str(num)) 6             encrypted_num = int(max_digit * len(str(num))) 7             total_sum += encrypted_num 8         return total_sum </pre>	<p>Uses <code>max(str(num))</code>, which returns the maximum character directly and handles positive integers correctly.</p>
Cluster $C_1$ — Fails on negative numbers (2 samples)	Key characteristic
<pre> 1 class Solution: 2     def sumOfEncryptedInt(self, nums: List[int]) -&gt; int: 3         total_sum = 0 4         for num in nums: 5             largest_digit = max([int(digit) for digit in str( 6                 num)]) 7             encrypted_num = int(str(largest_digit) * len(str( 8                 num))) 9             total_sum += encrypted_num 10        return total_sum </pre>	<p>Attempts to convert each character to an integer, raising <code>ValueError: invalid literal for int() with base 10: '-'</code> on negative inputs.</p>

### E.1.2 Problem abc332\_b: Glass and Mug

**Problem statement.** Given a glass with capacity  $G$  ml and a mug with capacity  $M$  ml, both initially empty, repeat  $K$  operations: (1) if the glass is empty, fill the mug completely; (2) else if the mug is empty, discard all water from the glass; (3) otherwise, transfer water from the mug to the glass (the glass fills completely if possible, with any remainder staying in the mug). Output the final water amounts in the glass and the mug.

**Cluster structure.** Two clusters with probabilities  $p_0 = 0.20$  (2 samples) and  $p_1 = 0.80$  (8 samples). Both clusters produce incorrect solutions, but with different error patterns.

Cluster $C_0$ — Wrong condition check (2 samples)		Key characteristic
<pre> 1 K, G, M = map(int, input().split()) 2 glass, mug = 0, 0 3 for _ in range(K): 4     if glass &lt; G: 5         glass = G 6     elif mug == 0: 7         mug = M 8     else: 9         transfer = min(mug, G - glass) 10        glass += transfer 11        mug -= transfer 12 print(glass, mug) </pre>	<p>Uses <code>glass &lt; G</code> instead of <code>glass == 0</code>, misinterpreting the problem requirements.</p>	
Cluster $C_1$ — Incorrect operation order (8 samples)		Key characteristic
<pre> 1 K, G, M = map(int, input().split()) 2 glass, mug = 0, 0 3 for _ in range(K): 4     if glass == 0: 5         mug = M 6     elif mug == 0: 7         glass = 0 8         empty it 9     else: 10        transferred = min(M - mug, glass) 11        mug += transferred 12        glass -= transferred 13 print(glass, mug) </pre>	<p>The glass is emptied when the mug is empty (line 6), so the glass always ends at 0.</p>	

## E.2 Case B: Partial Correctness Distinction

Case B isolates the contribution of inter-cluster distance under *identical* pass@1 outcomes: both tasks have pass@1 = 0 and admit the same 6/4 cluster split, yet differ substantially in partial\_pass@1. Distance-aware metrics recover this distinction; dispersion-only metrics cannot.

**Case B: Semantic Distance Explains Partial Correctness.** Table 18 presents a complementary scenario, where both tasks have pass@1 = 0 and induce identical execution cluster structure ( $M = 2$ , one cluster contains 6 programs, and the other 4 programs), yet differ substantially in partial\_pass@1.

Table 18: Case B: Metric-level comparison illustrating partial correctness under identical binary outcomes. Task 1 (abc326\_b) and Task 2 (3163) both have pass@1 = 0 and induce an identical  $M = 2$  cluster structure with sizes 6 and 4, but differ in their inter-cluster distance and therefore in partial\_pass@1.

Metric	Task 1 (Low-Distance)	Task 2 (High-Distance)	Diff.
pass@1	0	0	–
partial_pass@1	0.6667	0.0000	<b>0.6667</b>
Clusters	2 (6/4)	2 (6/4)	<b>0</b>
Distance	0.30	1.00	<b>0.70</b>
SDE	0.0720	0.2400	<b>0.1680</b>
DSDE	0.1800	0.6000	<b>0.4200</b>

In this case, dispersion-based signals provide no discrimination, as the two tasks share identical cluster structures and probabilities. However, the semantic distance between clusters differs markedly. The task with higher partial correctness exhibits smaller inter-cluster distances (e.g.,  $d_{01} = 0.30$ ), whereas the task with lower partial correctness shows much larger distances (e.g.,  $d_{01} = 1.00$ ). These differences align closely with the partial correctness outcomes and are faithfully reflected by distance-aware metrics.

### E.2.1 Problem abc326\_b: 326-like Numbers

**Problem statement.** A positive integer is a *326-like number* if it is a three-digit number satisfying (hundreds digit)  $\times$  (tens digit) = (ones digit). For example, 326, 400, and 144 are 326-like. Given a positive integer  $N$ , return the smallest integer  $\geq N$  that is a 326-like number.

**Cluster structure.** Two clusters with probabilities  $p_0 = 0.60$  (6 samples,  $\text{partial\_pass}@1 = 1.0$ ) and  $p_1 = 0.40$  (4 samples,  $\text{partial\_pass}@1 = 0.0$ ). The two clusters differ by an off-by-one ordering of the increment and the predicate check.

Cluster $C_0$ — Correct: check before increment (6 samples)	Key characteristic
<pre> 1 N = int(input()) 2 while True: 3     hundreds = N // 100 4     tens      = (N % 100) // 10 5     ones      = N % 10 6     if hundreds * tens == ones: # Check condition first 7         print(N) 8         break 9     N += 1                       # Then increment </pre>	<p>The predicate is checked before incrementing <math>N</math>, so the case in which <math>N</math> itself is already a 326-like number is handled correctly.</p>
Cluster $C_1$ — Off-by-one error (4 samples)	Key characteristic
<pre> 1 N = int(input()) 2 while True: 3     N += 1                       # Wrong: increment before 4     checking 5     hundreds = N // 100 6     tens      = (N % 100) // 10 7     ones      = N % 10 8     if hundreds * tens == ones: # Then check condition 9         print(N) 10        break </pre>	<p><math>N</math> is incremented before the predicate is checked, producing an off-by-one error whenever <math>N</math> itself is already a 326-like number.</p>

## E.2.2 Problem 3163: Subarrays Distinct Element Sum of Squares II

**Problem statement.** Given a 0-indexed integer array `nums`, the distinct count of a subarray is the number of distinct elements it contains. Return the sum of the squares of the distinct counts of all subarrays. For example, with `nums = [1, 2, 1]`, the answer is  $1^2 + 1^2 + 1^2 + 2^2 + 2^2 + 2^2 = 15$ .

**Cluster structure.** Two clusters with probabilities  $p_0 = 0.40$  (4 samples,  $\text{partial\_pass}@1 = 0.0$ ) and  $p_1 = 0.60$  (6 samples,  $\text{partial\_pass}@1 = 1.0$ ). The two clusters differ in *what* is being squared.

Cluster $C_0$ — Wrong: sums squared frequencies (4 samples)	Key characteristic
<pre> 1 from collections import Counter 2 class Solution: 3     def sumCounts(self, nums: List[int]) -&gt; int: 4         total = 0 5         n = len(nums) 6         for i in range(n): 7             count = Counter() 8             for j in range(i, n): 9                 count[nums[j]] += 1 10            # Wrong: sums (frequency^2), not (distinct 11            count)^2 12            total += sum(val ** 2 for val in count.values 13            ()) 14            return total </pre>	<p>Computes <math>\sum_k f_k^2</math>, where <math>f_k</math> is the frequency of element <math>k</math>, instead of (number of distinct elements)<sup>2</sup>—a fundamental misinterpretation of the specification.</p>
Cluster $C_1$ — Correct: squares the distinct count (6 samples)	Key characteristic
<pre> 1 class Solution: 2     def sumCounts(self, nums: List[int]) -&gt; int: 3         ans = 0 4         n = len(nums) 5         for i in range(n): 6             freq = {} 7             distinct_count = 0 8             for j in range(i, n): 9                 if nums[j] not in freq: 10                distinct_count += 1 11                freq[nums[j]] = 1 12            else: 13                freq[nums[j]] += 1 14            ans += distinct_count ** 2 # Correct: ( 15            distinct count)^2 16            return ans </pre>	<p>Tracks the number of distinct elements and squares this count, matching the specification.</p>

Across both cases, correctness differences cannot be explained by cluster counts or dispersion alone. Instead, they are driven by the magnitude of semantic distance between execution clusters. These examples provide concrete, intuitive evidence that the effectiveness observed in Section 4.2 arises from incorporating semantic distance, supporting the use of distance-aware uncertainty estimation for LLM-generated code.